CONSTRUCTING LUNAR NEUTRON FLUX MAPS WITH LRO/LEND NATURAL RESOLUTION.
T. A. Livengood[1], G. Chin[2], I. G. Mitrofanov[3], W. V. Boynton[4], J. G. Bodnarik[4], L. G. Evans[5], K. P. Harshman[4], M. L. Litvak[3], T. P. McClanahan[2], J. E. Murray[6], R. Z. Sagdeev[6], A. B. Sanin[3], R. D. Starr[7], J. J. Su[6] [1]CRESST/U. of Md, Code 693, NASA/GSFC, Greenbelt, MD 20771, timothy.a.livengood@nasa.gov, [2]NASA/GSFC, [3]Institute for Space Research, Moscow, Russia, [4]Lunar and Planetary Lab, U of Az, [5]Computer Sciences Corp., [6]Dept. of Physics, U. of Md, [7]Dept. of Physics, Catholic U. of America.

Introduction: Neutron detection rates within the Lunar Reconnainssance Orbiter (LRO) Lunar Exploration Neutron Detector (LEND) have been mapped in the Moon's polar regions, as well as globally [1–4]. Similar mapped measurements were acquired with the earlier Lunar Prospector Neutron Spectrometer (LPNS) [4,5]. Generally, these maps are constructed by identifying a measurement of neutron flux with a particular coordinate position on the Moon in order to build up a map of detection rates over each location. A spatial smoothing function can be applied to the mapped measurements in recognition of the finite spatial resolution of the detector system, which convolves emissions from a broad region into detections at a particular coordinate. Defining a convolution function for after-the-fact smoothing of a constructed map can pose difficulties, particularly in constructing a global map vs. a narrowly focused regional map. An alternative is to reconstruct every individual measurement of neutron flux as a convolution of emission sources and use this computationally expensive procedure to project the detection onto the surface as weighted contributions to the measurement. Successive projections over millions of neutron flux measurements enable constructing a global map at arbitrary sampling resolution that reflects the natural (intrinsic) spatial sensitivity of the instrument at the altitude of measurement. The result should be a global map of neutron flux from the Moon

The natural spatial resolution of an uncollimated neutron remote-sensing detector is controlled by the anisotropic emission of neutrons from a planetary surface into free space. The detector is sensitive to emission all the way out to the horizon, which distance varies according to the altitude of the spacecraft. Emission intensity declines with increasing slant angle relative to the surface normal, approximately proportional to cosine raised to a small power of order 1-1.5.

A collimated neutron detector, like the CSETN detector of LEND, complicates the matter. Detected neutrons include those that enter through the narrow field of view defined by the unobstructed collimated opening, as well as those that penetrate the necessarily finite opacity of the collimator wall [6]. Neutrons that successfully penetrate the collimator wall to reach the detector originate from the lunar surface at greater average energy than the population in collimation [7].

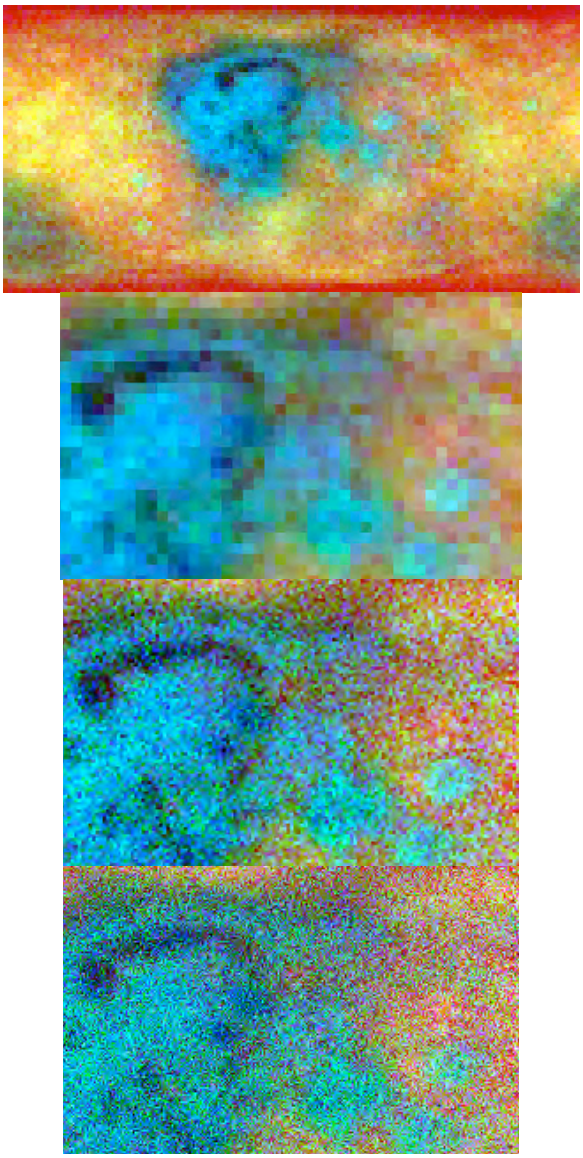

Fig. 1: Cylindrical-projection maps of lunar neutron emission at varying resolution, binning at 3°/pixel (*topmost*). Lower three maps zoom in on Eastern Maria region, at 3°/pixel (*top*), 1°/pixel (*center*), and 0.5°/pixel (*bottom*). Red represents thermal-energy neutrons (E < 0.4 eV); green represents low-energy epithermal neutrons (0.4 eV < E < ~10 keV); blue represents high-energy epithermal (HEE) neutrons (0.4 eV < E < 1 MeV).

Both collimated and uncollimated neutron flux populations are subject to anisotropic surface emission, but this effect will mainly constrain the resolution of the out-of-collimation component of the detected neutron population. Emission that is in collimation will originate from only a narrow range of emission angle. Detected flux arises from the superposition of these two neutron populations. Using ground calibration and modeled estimates for the contributions in and out of collimation, the goal of this work is to separate the superposed contributions as well as to extract the maximum information content from the uncollimated detectors.

LRO is in polar orbit, like LP before it, enabling the entire surface of the Moon to be mapped. The LRO data used here were acquired in 2009–2011, while the spacecraft was in circular orbit. The spatial density of measurements is greatest near the poles, least near the equator. The maps in Fig. 1 use cylindrical projection, the natural distribution for polar-orbital measurements since the spacecraft spends equal time in each interval of latitude and longitude in circular orbit (Fig. 2). The planned projection method should work equally well for the elliptical orbit that LRO has occupied since 2011, but the present effort will begin with the circular orbit data. In elliptical orbit, the projection onto the surface of the angular sensitivity will vary with altitude. Variations with altitude also occur during the nominally circular orbit phase and will be taken into account in the planned work.

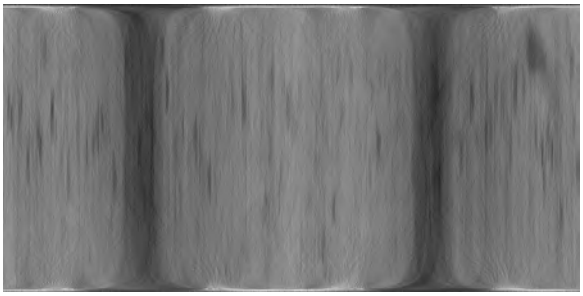

Fig. 2: Cylindrical-projection map of dwell time per map element for the LEND CSETN collimated detector, 0.5°/pixel. Dark meridians show longitude range at which LEND was sometimes deactivated to accommodate LRO motor firing.

Inspection of the maps in Fig. 1 shows that actual resolution improves in the transition from coarse sampling to fine sampling, at the edges of features in the Maria and large craters. Unfortunately, noise also increases as map elements become smaller and fewer measurements contribute to the flux estimate at each location. The distinction between a noise fluctuation and possible actual variability becomes ambiguous. At even finer sampling, gaps appear at mid- and low latitudes in regions that the spacecraft did not directly pass over. This work will paint the map with a measurement value weighted according to the estimated resolution of each detector so that a map can be built with fine resolution and no gaps while acknowledging that the actual region contributing to the measurement is broad, stretching out to ~3° FW-at-half-power at the equator. This process should reduce noise similar to the 3° binning, while permitting narrow features of smaller scale to be preserved at the natural resolution of the instrument.

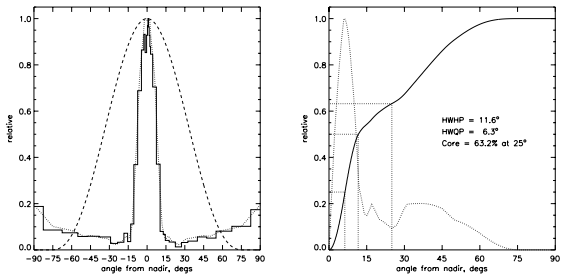

Fig. 3: Angular sensitivity of LEND collimated detector [6]. (*left*) Measured angular sensitivity (histogram) and estimated anisotropic emission rate from lunar surface (dashed). (*right*) Convolution of angular sensitivity with anisotropic emission and annular surface area (dotted), with integrated signal interior to radial distance from subspacecraft point (solid).

References: [1] Mitrofanov *et al.* (2010) *Science* **330**, 483–486.s [2] Sanin *et al.* (2012) *JGR-Planets* **117**, E00H26. [3] Litvak *et al.* (2012a) *JGR-Planets* **117**, E00H22. [4] Livengood *et al.* (2016) *Icarus*, in review. [5] Maurice *et al.* (2004) *JGR-Planets* **109**, E07S04. [6] Litvak *et al.* (2012b) *JGR-Planets* **117**, E00H32. [7] Livengood *et al.* (2015) *Icarus* **255**, 100–115.